Hybridization Effects and Metallicity in Small Radius Carbon Nanotubes

X. Blase, Lorin X. Benedict, Eric L. Shirley,* and Steven G. Louie

*Department of Physics, University of California at Berkeley and Materials Sciences Division,
Lawrence Berkeley Laboratory, Berkeley, California 94720*

Hybridization of the σ^* and π^* states of the graphene network is shown to be as important as band-folding effects in determining the metallicity of small radius carbon nanotubes. Using detailed plane-wave *ab initio* pseudopotential local density functional (LDA) calculations, we find that the electronic properties of small tubes are significantly altered from those obtained in previous tight-binding calculations. Strongly modified low-lying conduction band states are introduced into the band gap of insulating tubes because of strong σ^*-π^* hybridization. As a result, the LDA gaps of some tubes are lowered by more than 50%, and a tube previously predicted to be semiconducting is shown to be metallic.

Since the discovery of graphitic nanotubes [1] in carbon rods under arc discharge, many experimental and theoretical efforts have focused on the properties of these novel quasi-one-dimensional structures. Classifications of the tubes as metals or semiconductors were given [2,3] on the basis of how the underlying graphite band structure is "folded" when one applies the tubes' azimuthal periodic boundary conditions. Although early work [2–4] has noted that hybridization of the graphitic σ, π, π^*, and σ^* states should occur because of the curvature of the tubes, the importance of these effects was not fully appreciated. The tube states near the Fermi level were described as chiefly π and π^* states. Recently [5], nanotubes with very small radii were experimentally produced, with diameters as small as 7 Å. In this Letter, we show that sufficiently strong hybridization effects occur in such tubes which dramatically change the band structure proposed in previous works.

We have carried out both *ab initio* pseudopotential local density function (LDA) calculations and Slater-Koster [6] tight-binding (TB) calculations. Following the notation of Ref. [3], we study the tubes $(n,0)$, with n ranging from 6 to 9. As illustrated in Fig. 1(a), tube $(n,0)$ corresponds to wrapping a section of a graphitic sheet in the indicated orientation with n hexagons around the tube circumference. The diameter of these tubes ranges from 4.78 Å for $(6,0)$ to 7.20 Å for $(9,0)$. The LDA electronic structure calculations were performed using a plane-wave basis set. We generated first a semilocal pseudopotential following the scheme of Troullier and Martins [7] and made it fully nonlocal according to the Kleinman and Bylander procedure [8]. The energy cutoff for the electronic wave functions was set at $E_{cut} = 49$ Ry, leading to a 0.05 eV convergence of the band energies. The very large number of plane waves needed for this type of calculation [ranging from 13500 for $(6,0)$ to 19000 for $(9,0)$] required the use of an efficient iterative diagonalization scheme [9]. The LDA calculations were carried out in a supercell geometry with a hexagonal array of tubes, with the closest distance between atoms on different tubes being 5.5 Å. This permitted the neglect of

tube-tube interactions. For the TB calculations, we used the first and second nearest neighbor parameters proposed in Ref. [10] for graphite.

Along the axes of the tubes, the length of the unit cell was set by assuming that the tube was generated simply by rolling a graphite sheet segment [2]. Using the Hellmann-Feynman theorem, we found that the stresses imposed on each supercell were negligible in the axis direction. The most important structural change was the tendency of the tube to reduce its radius from that given by the above rolling. This effect was nonetheless small, ranging from 1.6% reduction for $(6,0)$ to nearly zero for $(9,0)$. We found similar results within a tight-binding total energy minimization scheme [11]. The effect of this relaxation on the electronic band structure was negligible. We also relaxed the internal coordinates of the atoms using Hellmann-Feynman forces. The forces were very small, and all the atoms remained equivalent within the unit cell.
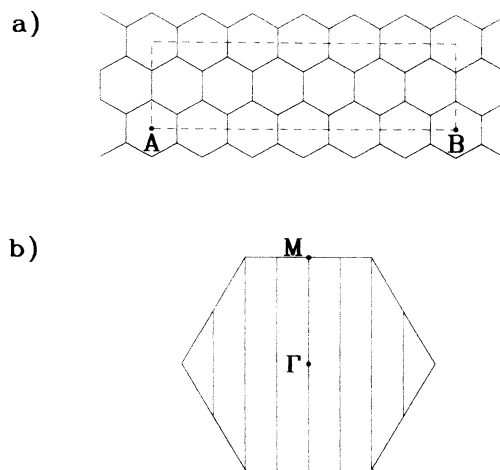
a)

b)

FIG. 1. (a) Unit cell of the $(6,0)$ tube mapped onto the graphite sheet. For the tube, point A is rolled onto point B. (b) Brillouin zone of the graphite sheet. The vertical lines mark the set of allowed k vectors for the tube.

TABLE I. Band gap (in eV) of selected tubes. All gaps given are direct and at the Γ point. For the metallic case, the overlap of the bands is given as a negative gap.

Tube	Tight binding Ref. [2]	Present calculations TB	LDA
(6,0)	$\sim$0.2	0.05	Metal ($-$0.83)
(7,0)	$\sim$1	1.04	0.09
(8,0)	1.22	1.19	0.62
(9,0)	0.04	0.07	0.17

Our results for the band gaps are given in Table I, compared with those from previous TB work [2]. We find major differences between the results from LDA and the TB calculations. The most significant difference occurs for the tube (6,0) which has been previously predicted to be a small gap semiconductor [2]. We find in this work that, within LDA, tube (6,0) is a metal. In addition, we find that tubes (7,0) and (8,0) are semiconductors, consistent with previous calculations, but with a much smaller gap than those from TB based works. This discrepancy is mainly due to a singly degenerate state which is much lower in our LDA calculations than in the TB work. We know that LDA is known to underestimate the value of the band gap of many materials, but the narrowing of the gap here is due primarily to curvature effects, as evidenced by the dependence on tube size.

In Fig. 2 we show the band structure and density of states (DOS) for the tube (6,0). The singly degenerate state mentioned above is labeled by (a). At γ, this state

is 0.83 eV below the doubly degenerate state that forms the top of the valence band in TB calculations. This band overlap makes the tube (6,0) a metal within LDA with a density of states at the Fermi level equal to $D(E_F) = 0.07$ state/eV atom. For this tube, we also performed an independent LDA calculation using a semilocal pseudopotential and another diagonalization scheme as described in Ref. [12]. The two LDA band structures were in excellent agreement. We also checked that this state is insensitive to the small structural relaxation effects described above.

As we shall show, state (a) occurs in all $(n,0)$ tubes for symmetry reasons, but its energy at Γ varies with n. For the tubes (7,0) and (8,0), state (a) does not close the gap but reduces significantly its value as compared to TB calculations. For these two tubes, the state (a) at Γ lies between the two doubly degenerate states that form the highest occupied and lowest unoccupied molecular orbital states in TB calculations. This state reduces the TB gap by 1 eV for (7,0) and by 0.6 eV for (8,0). For the tube (9,0), the state (a) lies just above the TB lowest unoccupied molecular orbital state and therefore does not fall within the gap.

The discrepancy between TB and LDA calculations decreases as the radius of the tube increases. This is consistent with the notion that, in large tubes with small curvatures, one obtains a good description of the nanotube band structure by "folding" the graphite sheet band structure. However, this idea implicitly relies on the assumption that states around the gap or Fermi level are essentially π or π^* derived [3,4]. This is not true for small tubes where the curvature is so strong that large hybridization effects occur. We show in Fig. 3 the charge density distribution for the state (a) at Γ for the tube (6,0). One can see that most of the wave function is localized outside the tube. If this state is mostly π or π^* derived, it should have equal weight inside and outside the tube. Detailed analysis of the σ^*-π^* hybridization in $(n,0)$ tubes also indicates that this state should be mostly
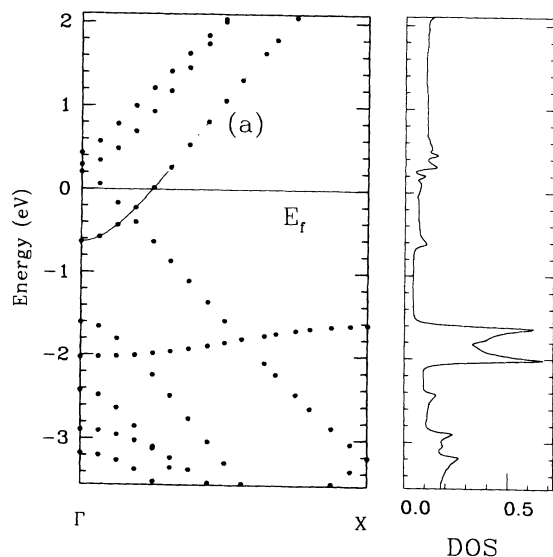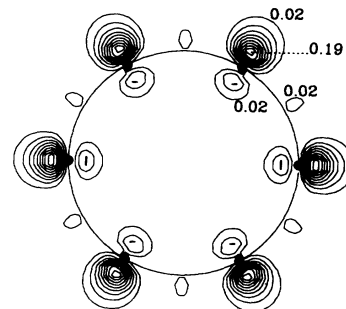

FIG. 2. Band structure and density of states (states/eV atom) for the tube (6,0). The energies are in eV and the zero is at the Fermi level. We trace the new band (a) around the center of the Brillouin zone as a guide to the eye.

FIG. 3. Contour plot of the charge density for state (a) at Γ for tube (6,0). The contours are in a plane perpendicular to the axis of the tube which contains six carbon atoms. The numbers quoted are in units of $e/(\text{a.u.})^3$. The circle represents a cross section of the cylinder on which the atoms lie.

outside of the tubes for k vectors near the tube's zone center. We show below that it is crucial to accurately describe the σ^* states and their interaction with the π^* complex before one is able to reproduce within TB the behavior of the state (a) in our LDA calculation.

To study the effects of hybridization on the state (a) of tube (6,0), we begin with a planar sheet of graphite with the unit cell described in Fig. 1(a). Because state (a) is singly degenerate, in the "band-folding" language, it must be derived from the Γ-M line of the graphite sheet Brillouin zone (BZ), and must occur in all $(n,0)$ tubes. As a result of the boundary conditions of the tube, M is folded onto Γ. We plot in Fig. 4(a) the corresponding TB bands along the Γ-X direction of the tube (see Ref. [2]). From the symmetry of the tube, singly degenerate states only mix with each other and not with states of higher degeneracy, so only these need be considered in the analysis of the behavior of state (a). The dashed lines are the singly degenerate bands coming from the folding of the π^* and σ^* graphite bands along the Γ-M line of the hexagonal graphite BZ [Fig. 1(b)] onto the Γ-X line of the tube BZ. Next we bend this graphite sheet along the AB direction while imposing the proper periodic boundary conditions in order to mimic a continuous transformation of the graphite sheet onto the (6,0) tube. This procedure distinguishes the zone-folding effects from the curvature effects.

Figure 4 illustrates the evolution of our TB band structure under this transformation for two of these "intermediate" structures. Their radii of curvature are between $R = \infty$ of planar graphite [Fig. 4(a)] and $R = 2.39$ Å of tube (6,0) [Fig. 4(d)]. For a curved sheet of graphite, the π^* and σ^* states mix and repel each other, resulting in a lowering in energy of the (originally) purely π^* states. It is the lower hybridized π^* band which gives rise to the singly degenerate state (a) near E_F in the LDA calculation. Therefore, within the TB Hamiltonian of Ref. [10], this state does exist, but it is not low enough in energy to make the tube metallic as found in the LDA calculation. We note also that, with a localized basis set limited to $2s$ and $2p$ orbitals, TB calculations are unable to describe large charge transfer asymmetrically away from the atoms. However, in our LDA calculations, we find the total potential to be locally symmetric inside and outside the tube so that the localization of the state (a) outside the tube must be mainly due to hybridization and not electrostatic effects. Similar studies have been made for tubes (7,0), (8,0), and (9,0), yielding similar results.

Some workers [13,14] have recently suggested that very small radius tubes may not be energetically stable. It is argued that at some critical radius the elastic strain energy per atom stored in the rolled sheet would be larger than the dangling bond energy per atom for the flat graphitic strip obtained by "cutting" the tube along its cylindrical axis. In order to address this question for the tubes of our study, we carried out LDA total energy calculations for our smallest tube (6,0) with radius 2.39 Å, and its corresponding strip and found that the tube is energetically more stable than the strip. This implies that the critical radius below which tube energy exceeds strip energy for $(n,0)$ tubes is less than the (6,0) radius. The result is in agreement with the conclusion of a previous classical force-field calculation [14] which predicts the critical radius to be ~ 2 Å, in contradiction with the semiempirical calculation of Ref. [13] which predicts ~ 3.85 Å. However, we stress that as long as the tube and strip energies are comparable, kinetic effects will still dominate the growth process. Thus, total energy comparisons may not be relevant to the question of tube formation.

In conclusion, large π^*-σ^* hybridization effects can occur in small nanotubes which drastically change the electronic band structure from that obtained by simply "folding" the graphite sheet band structure. These effects are demonstrated in our study of tubes (6,0) to (9,0), some of which are comparable in size to the smallest tube experimentally observed thus far. Our results show that, for this class of tubes, hybridization effects change the energy and character of the lowest lying conduction band states with important consequences to the metallicity and transport properties of the tubes. An implication of this result is that hybridization effects could also play an important role in doped small nanotubes with metallic dopants either inside or on the tubes.
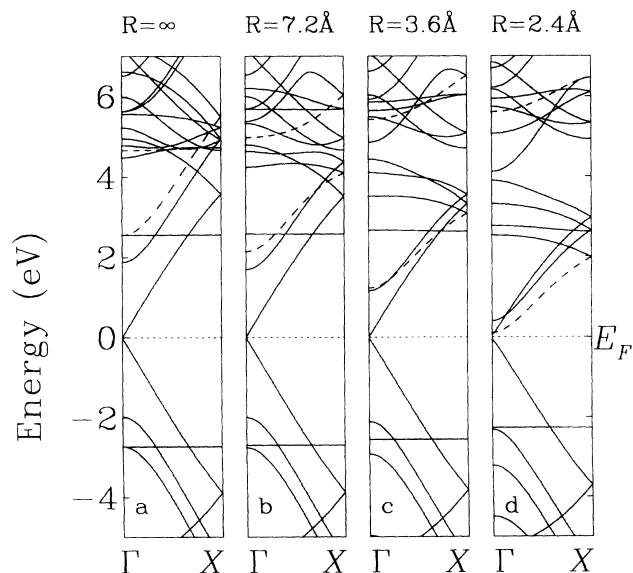
FIG. 4. Evolution of the graphite TB bands near the Fermi level for the (6,0) geometry under increasing curvature. Energies are in eV and the zero is set at the Fermi level. The dashed curves mix strongly with each other due to curvature. In an LDA calculation, the lower one would span the gap. The radii of curvature are indicated.

*Permanent address: Lawrence Livermore National Laboratory, Livermore, CA 94551.

[1] S. Iijima, Nature (London) **354**, 56 (1991).

[2] N. Hamada, S. Sawada, and A. Oshiyama, Phys. Rev. Lett. **68**, 1579 (1992).

[3] R. Saito, M. Fujita, G. Dresselhaus, and M. S. Dresselhaus, Appl. Phys. Lett. **60**, 2204 (1992).

[4] J. W. Mintmire, B. I. Dunlap, and C. T. White, Phys.

Rev. Lett. **68**, 631 (1992).

[5] S. Iijima and T. Ichihashi, Nature (London) **363**, 603 (1993); D. S. Bethune *et al.*, Nature (London) **363**, 605 (1993).

[6] J. C. Slater and G. F. Koster, Phys. Rev. **94**, 1498 (1954).

[7] N. Troullier and J. L. Martins, Solid State Commun. **74**, 613 (1990).

[8] L. Kleinman and D. M. Bylander, Phys. Rev. Lett. **48**, 1425 (1982).

[9] N. Troullier and J. Martins, Phys. Rev. B **46**, 1754 (1992).

[10] D. Tománek and S. G. Louie, Phys. Rev. B **37**, 8327 (1988).

[11] C. H. Xu, C. Z. Wang, C. T. Chan, and K. M. Ho, J. Phys. Condens. Matter **4**, 6047 (1992).

[12] E. L. Shirley and S. G. Louie, Phys. Rev. Lett. **71**, 133 (1993).

[13] A. A. Lucas, P. H. Lambin, and R. E. Smalley, J. Phys. Chem. Solids **54**, 587 (1993).

[14] S. Sawada and N. Hamada, Solid State Commun. **83**, 917 (1992).